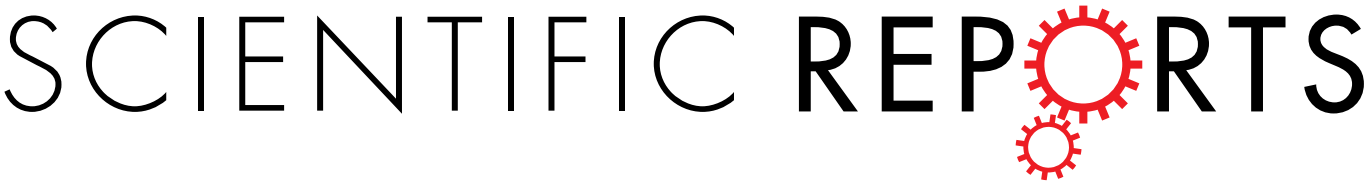

OPEN

Formation and evolution of orientation-specific CO_2 chains on nonpolar ZnO(10$\bar{1}$0) surfaces

Received: 16 November 2016
Accepted: 23 January 2017
Published: 06 March 2017

Yunjun Cao, Min Yu, Shandong Qi, Tingting Wang, Shiming Huang, Shujun Hu, Mingchun Xu & Shishen Yan

Clarifying the fundamental adsorption and diffusion process of CO_2 on single crystal ZnO surfaces is critical in understanding CO_2 activation and transformation over ZnO-based catalysts. By using ultrahigh vacuum-Fourier transform infrared spectroscopy (UHV-FTIRS), we observed the fine structures of CO_2 vibrational bands on ZnO(10$\bar{1}$0) surfaces, which are the combinations of different vibrational frequencies, originated from CO_2 monomer, dimer, trimer and longer polymer chains along [0001] direction according to the density functional theory calculations. Such novel chain adsorption mode results from the relatively large attractive interaction between CO_2 and Zn_{3c} atoms in [0001] direction. Further experiments indicate that the short chains at low coverage evolve into long chains through Ostwald ripening by annealing. At higher CO_2 coverage (0.7 ML), the as-grown local (2 × 1) phase of chains first evolve into an unstable local (1 × 1) phase below 150 K, and then into a stable well-defined (2 × 1) phase above 150 K.

CO_2 activation and transformation are the key steps in CO_2 utilizations such as in environment protections and renewable energy fields. One famous example about CO_2 utilization is the methanol synthesis over Cu/ZnO/Al_2O_3 catalysts by syngas ($CO/CO_2/H_2$) industrially[1–4]. In the three-way catalyst, ZnO plays a pivotal role in CO_2 activation and stabilization[2], however, to elucidate the underlying mechanism of CO_2 activation at the molecular level, studies on well-defined single crystal ZnO surfaces under ultrahigh vacuum (UHV) conditions are essential[5,6]. The nonpolar mixed-terminated ZnO(10$\bar{1}$0) surface is the energetically most favorable surface and dominates the exposed surfaces of ZnO particles in applications[3,7]. Therefore, the investigation of CO_2 adsorption and activation behavior on ZnO(10$\bar{1}$0) surfaces is typical and helpful in understanding of the ZnO-catalyzed CO_2 chemistry.

The mixed-terminated ZnO(10$\bar{1}$0) surface is composed of rows of ZnO "dimers" separated by trenches along [1$\bar{2}$10] direction. The ZnO "dimer" consists of one threefold coordinated surface Zn cation (Zn_{3c}) and the adjacent surface O anion (O_{3c}), running along the crystallographic [0001] direction[8,9]. An early near edge X-ray absorption fine structure (NEXAFS) study suggested a bidentate adsorption configuration of CO_2 on ZnO(10$\bar{1}$0) surfaces[10]. Later, the high resolution electron energy loss spectroscopy (HREELS) results together with density functional theory (DFT) calculations[5] supported an unusual tridentate carbonate configuration: the middle C-atom bound to the surface O_{3c} anion and the two end O-atoms of CO_2 molecule bound to two surface Zn_{3c} cations along [0001] direction. Besides, experiments also observed two ordered carbonate adlayers: the close packed (1 × 1) phase corresponds to 1 ML CO_2 coverage, and the open (2 × 1) phase to 0.5 ML[5]. (Here, 1 ML is defined as the density of the surface Zn_{3c} cations on the clean surface.) In the (2 × 1) phase, the free surface Zn_{3c} sites were found surprisingly to bind CO more strongly due to charge transfer, which suggests the potential importance of such open phase in the polybasic catalytic reactions such as methanol synthesis from syngas[11,12].

Up to date, only the tridentate carbonate configuration, and the ordered (2 × 1) and (1 × 1) phases are reported for CO_2 on ZnO(10$\bar{1}$0)[5,6–11]. We wonder how the initial CO_2 tridentate carbonates evolve into the ordered adlayers? What is the mechanism behind the evolution from tridentate carbonates to the ordered adlayers? Monitoring the molecular vibration of adsorbed CO_2 is an important way to clarify such evolution process, since the molecular vibration is very sensitive to the chemical surrounding change of the adsorbed molecules. For instance, by using infrared spectroscopy, Heidberg *et al.* studied the dynamic dipole-dipole-coupling of adjacent CO_2

School of Physics, State Key Laboratory of Crystal Materials, Shandong University, 27 Shanda Nanlu, Jinan, Shandong 250100, P. R. China. Correspondence and requests for materials should be addressed to S.H. (email: hushujun@sdu.edu.cn) or M.X. (email: xumingchun@sdu.edu.cn)

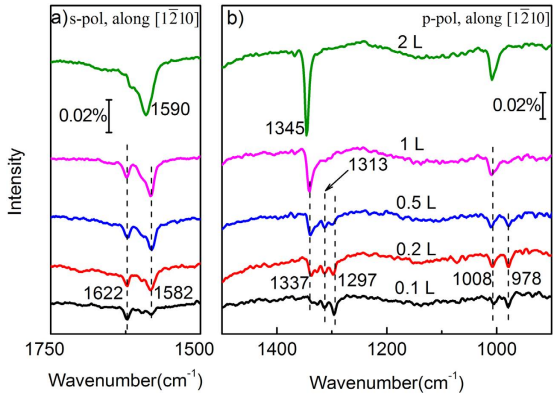

Figure 1. IRRA spectra of CO_2 adsorbed on ZnO(10$\bar{1}$0) surfaces as a function of CO_2 dosage by using (**a**) s-polarized and (**b**) p-polarized IR beams, respectively. The IR light incident is along [1$\bar{2}$10] direction. All spectra were acquired at 90 K.

molecules on MgO(100) and NaCl(100) surfaces[13–16]. Similar results were reported for CO_2 adsorption on rutile TiO_2(110) surfaces in our previous work[17]. On the ZnO(10$\bar{1}$0) surface, using the high resolution ultrahigh vacuum-Fourier transform infrared spectroscopy (UHV-FTIRS), Buchholz *et al.* characterized the ordered (2×1) phase at high CO_2 coverage[6], but they did not observe the evolution from the initial tridentate carbonates to the ordered adlayers.

In this paper, based on the high resolution UHV-FTIRS and DFT calculations, we reported the fine structures combined by of CO_2 vibrational levels on ZnO(10$\bar{1}$0) surfaces with increasing CO_2 coverage, which are attributed to the formation of [0001]-oriented short CO_2 polymer chains consisting of monomer, dimer, trimer and so on. The as-grown chains at high CO_2 coverage further evolve into the unstable local (1×1) phase below 150 K, and then relax into the stable (2×1) phase above 150 K.

Results and Discussion

Figure 1 presents the polarized infrared reflection absorption spectroscopy (IRRAS) data of adsorbed CO_2 on ZnO(10$\bar{1}$0) surfaces at 90 K with IR light incident along [1$\bar{2}$10] direction. At the initial adsorption with 0.1 L (1 L = 1.33×10^{-6} mbar·s) CO_2 dosage, one vibrational band at 1622 cm^{-1} first appears in s-polarized spectra (Fig. 1a); in p-polarized spectra, two bands at 1297 and 978 cm^{-1} (Fig. 1b) emerge simultaneously. These dramatically lowered vibration frequencies of adsorbed CO_2 relative to that of gas-phase CO_2 (2349 cm^{-1}) demonstrate evidently that CO_2 have chemically adsorbed on ZnO(10$\bar{1}$0) surfaces. Based on the IR judgement principle on dielectric substrates[17,18], the vibrational bands at 1622, 1297 and 978 cm^{-1} for CO_2 on ZnO(10$\bar{1}$0) surfaces are assigned respectively to the asymmetrical stretching mode (ν_{as}(OCO), in-plane), symmetrical stretching mode (ν_s(OCO), out-of-plane) and the stretching vibration between the carbon atom and the underneath surface O_{3c} atom ($\nu(CO_{3c})$, out-of-plane) for tridentate carbonates. (See Figure S1 for the detailed judgements of the CO_2 vibration direction through the polarized IRRAS.) Our assignment is in accordance with previous HREELS and FTIR reports[5,6–19].

It is interesting that we observed the fine structures of adsorbed CO_2 vibrational levels with increasing CO_2 coverage. For ν_{as} vibration, besides the 1622 cm^{-1} band (Fig. 1a), a new band appears at 1582 cm^{-1}, and they finally converge into one intense band at 1590 cm^{-1} for saturated CO_2 coverage (2 L). Simultaneously, for ν_s vibration (Fig. 1b), besides the 1297 cm^{-1} band, 1313 and 1337 cm^{-1} bands appear and finally evolve to one sharp 1340 cm^{-1} band. The $\nu(CO_{3c})$ band evolves from 978 cm^{-1} to 1008 cm^{-1} gradually. Therefore, we can divide the fine structures of tridentate carbonate vibration into four different groups as shown in Fig 1: I 1622, 1297, 978 cm^{-1}; II 1582, 1313, 978 cm^{-1}; III 1582, 1337, 1008 cm^{-1}; IV 1590, 1345, 1008 cm^{-1}, which correspond to four configurations of tridentate carbonates. It is clear that the frequencies of the same vibrational modes in different CO_2 configurations are well distinguished except a few vibrational modes at 978, 1008 and 1582 cm^{-1}.

To examine whether the fine structures of CO_2 vibration is associated with the surface defects, we treated the ZnO(10$\bar{1}$0) surface in atomic oxygen atmosphere of 2×10^{-6} mbar at 750 K and 10 L O_2 at 90 K, but no change in the fine structures is observed. Therefore, the prepared ZnO(10$\bar{1}$0) surface can be regarded as the stoichiometric surface with negligible surface defects. Recent STM studies also reported that no apparent oxygen vacancies or miss zinc-oxygen dimers were observed on the vacuum-annealed ZnO(10$\bar{1}$0) surface[20]. Actually, the fine structures of molecular vibrations have already been observed on some single crystal substrates, such as CO and CO_2 on MgO(100) and NaCl(100), which were attributed to the dipole-dipole-coupling in ordered molecular layers[13–16] instead of the influence of the surface defects.

To clarify the interaction between CO_2 on ZnO(10$\bar{1}$0), different configurations of two carbonates were designed and checked by DFT calculations. We first calculated the structure of CO_2 monomer on the ZnO(10$\bar{1}$0) surface of a (2×4) supercell with the long axis along [0001] direction. As shown in Fig. 2a, the tridentate configuration was confirmed, which is in well agreement with previous calculation results[5]. Then three distinct configurations of two CO_2 molecules were calculated. The results reveal that when two CO_2 form a chain along [0001]

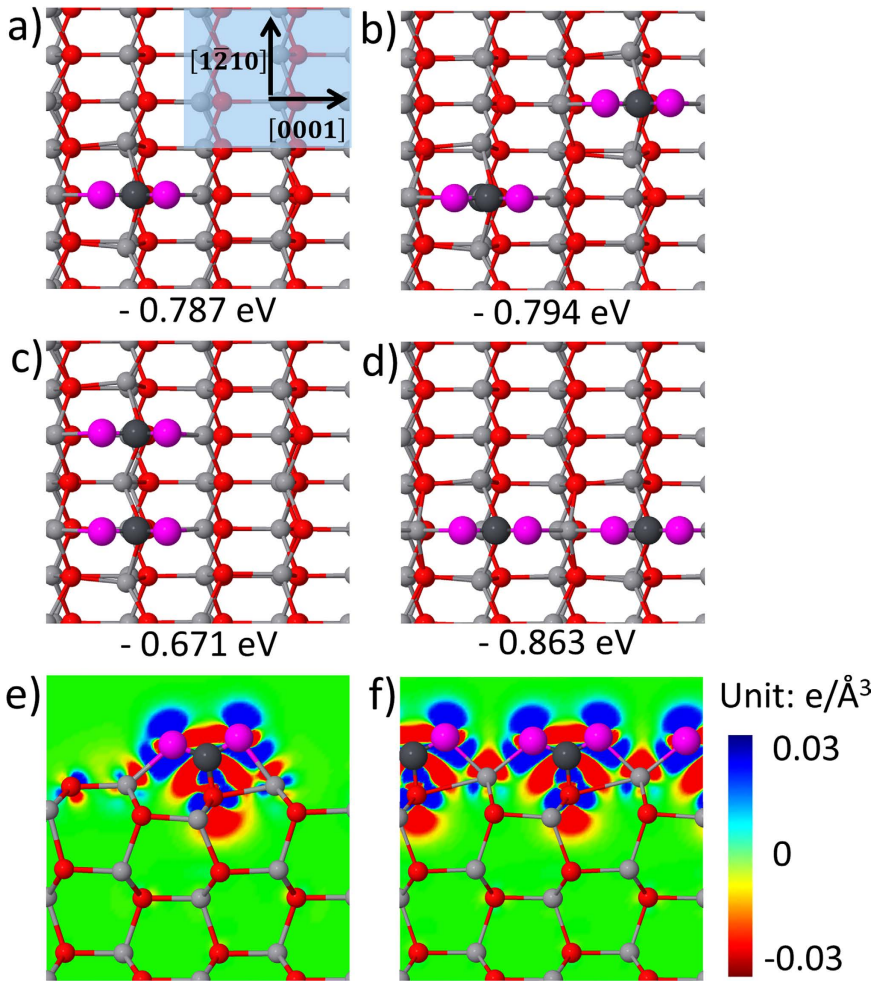

Figure 2. Different distributions for CO_2 molecules on ZnO(10$\bar{1}$0) surfaces and their DFT-calculated binding energies. (**a**) single CO_2 molecule, (**b**) two CO_2 in diagonal, (**c**) two adjacent CO_2 along [1$\bar{2}$10] direction and (**d**) two adjacent CO_2 along [0001] direction. The binding energy for each configuration is given in eV per CO_2 molecule, where the negative energy means the adsorption is exothermic. Charge density difference maps for (**e**) single CO_2 molecule and (**f**) CO_2 chains along [0001] direction. Electron accumulation and depletion regions are shown in blue and red, respectively. Panels (**a**–**d**) represent the top view and panels (**e**,**f**) for the side view.

direction, the binding energy per molecule is the lowest, corresponding to the most stable configuration compared to the other distributions of the two CO_2. The similar results were also calculated in a recent literature[21].

Based on the above calculation result, we designed CO_2 molecular chains with different length on the ZnO(10$\bar{1}$0) surfaces of a (6 × 2) supercell and calculated the corresponding vibrational frequencies. The chain contains, respectively, one, two, three, four, five and infinite carbonates arraying end to end along the long axis [0001] direction. All the results are shown in Table 1. We can see that the calculated 1585 cm^{-1}, 1261 cm^{-1} and 958 cm^{-1} for the monomer respectively correspond to the experimental results of Group I: 1622 cm^{-1}, 1297 cm^{-1} and 978 cm^{-1}. Thus the bands of Group I are assigned to the carbonate monomer vibrations. It is easy to understand that most CO_2 are diluted at the initial adsorption on the surface to form carbonate monomers.

As shown in Table 1, the ν_{as} dramatically redshifts from 1585 cm^{-1} of the monomer to 1546 cm^{-1} of the dimer, and it slightly changes from 1546 to 1540 cm^{-1} with increasing CO_2 from dimer to pentamer. Further lengthening the chain to infinite, the ν_{as} blueshifts back to 1563 cm^{-1}. On the contrary, the ν_s of monomer to pentamer increases monotonously from 1261 to 1302 cm^{-1}, and further to 1310 cm^{-1} for infinite length. The evolution trend of the calculated results is well consistent with our experimental IR frequencies. Therefore, the fine structures of CO_2 vibrations originate from the short CO_2 chains composed of monomer, dimer, trimer and so on when dosing CO_2 from 0.1 L to 1 L. Accordingly, in Table 1 the strong bands of Group IV measured at saturated CO_2 dosage (2 L) are assigned to the infinitely long chain vibrations.

Generally, the one-dimensional chain formation requires the symmetry loss of substrate surfaces[22], such as trenches[23,24] or steps[25,26] on surfaces along specific direction, i.e., the space restriction plays a major role in the chain formation. However, on ZnO(10$\bar{1}$0) surfaces, the CO_2 chains are along [0001] direction, rather than along the surface trench direction [1$\bar{2}$10]. To explore the formation mechanism of such CO_2 chains, we performed the

		Theory			Experimenta		
		$\nu_{as}(cm^{-1})$	$\nu_{s}(cm^{-1})$	$\nu(cm^{-1})$	$\nu_{as}(cm^{-1})$	$\nu_{s}(cm^{-1})$	$\nu(cm^{-1})$
CO_2 chain	Monomer	1585	1261	958	1622	1297	978
	Dimer	1546	1280	984/951	1582	1313	1008/978
	Trimer	1542	1290	984/950	1582	1320	1008/978
	Tetramer	1541	1298	987/981/976/955	1582	1337	1008/978
	Pentamer	1540	1302	986/982/978/976/949			
	infinite chain	1563	1310	980	1590	1345	1008
chains distribution	isolated	1567	1303	976			
	spacing	1574	1303	968	1590	1345	1008
	neighbouring	1593	1309	966	1618	1345	1001

Table 1. Calculated vibrational frequencies of CO_2 in different configurations and distributions on ZnO(10$\bar{1}$0) surfaces. The corresponding experimental values are also listed for comparison.

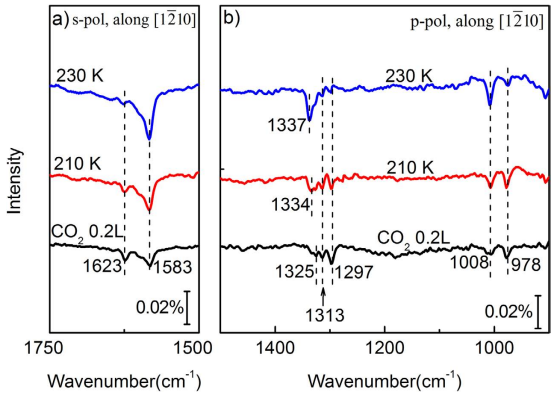

Figure 3. IRRA spectra of 0.2 ML CO_2 adsorbed on ZnO(10$\bar{1}$0) surfaces with annealing by using (**a**) s-polarized and (**b**) p-polarized IR beams, respectively. The IR light incident is along [1$\bar{2}$10] direction. All spectra were acquired at 90 K.

charge transfer analysis of CO_2 monomer and CO_2 chains on ZnO(10$\bar{1}$0) surfaces by DFT calculations. The calculated charge density difference maps are shown in Fig. 2e and f, respectively. The bonding formation obviously bents the linear CO_2 and induces the charge redistribution. In the single carbonate, as shown in Fig. 2e, the two O atoms of CO_2 get more electrons while the C and Zn_{3c} atoms lose more electrons. The charge redistribution induces the extra Coulomb attraction between Zn_{3c} atoms and O atoms of CO_2. For the carbonate chain, as shown in Fig. 2f, two O atoms bond to one Zn_{3c} atom, and the induced positive electricity of Zn_{3c} atoms is evidently enhanced. As a result, the extra attractive Coulomb interaction between Zn_{3c} atoms and O atoms of CO_2 is strongly enhanced. Such enhanced attractive interaction makes the chain configuration of adsorbed CO_2 along [0001] direction more stable. Along [1$\bar{2}$10] direction, on the contrary, the enhanced electrostatic repulsion between CO_2 molecules causes the CO_2 alignment along [1$\bar{2}$10] direction less stable.

To understand the phase evolution of CO_2 adlayers on ZnO(10$\bar{1}$0), the temperature dependence of CO_2 chains was studied for fixed CO_2 coverages. For the low CO_2 coverage of 0.2 ML (corresponding to 0.2 L), the IRRAS results are shown in Fig. 3. Slowly annealing to 230 K, the ν_{as} band at 1623 cm^{-1} gradually converts to 1583 cm^{-1} in Fig. 3a. At the same time, the three close peaks (1297, 1313, 1325 cm^{-1}) of ν_s finally convert to one peak at 1337 cm^{-1}, and the 978 cm^{-1} band to 1008 cm^{-1} band, as shown in Fig. 3b. (The corresponding p-polarized spectra with IR light incident along [0001] direction can be seen in Figure S2 in the SI.) Such band conversions reveal that the chain conversions from the monomer to long chains happened upon annealing through Ostwald ripening. Our present study provides an effective way to synthetize long CO_2 chains along [0001] direction on ZnO(10$\bar{1}$0) surfaces.

For the high coverage of 0.7 ML (corresponding to 2 L), the IRRAS results with annealing are shown in Fig. 4a and b. As mentioned before we have assigned the 1590 cm^{-1} to the ν_{as} and 1345 cm^{-1} to the ν_s of long CO_2 chains at 90 K. Slowly annealing to 150 K, the ν_{as} band at 1590 cm^{-1} unexpectedly converts to 1618 cm^{-1} gradually, as shown in Fig. 4a. Further annealing to 240 K, the band gradually redshifts back to 1590 cm^{-1}. On the other hand, the ν_s band (1345 cm^{-1}) keeps constant from 90 K to 150 K. Over 150 K, its intensity slightly decreases with a weak redshift. (The corresponding p-polarized spectra with IR light incident along [0001] direction can be seen in Figure S3 in the SI). It is easy to know that for the high CO_2 coverage and relative high annealing temperature, the length change of a single long chain will not induce such obvious changes of the CO_2 vibration frequencies. But the change of the separated distance along [1$\bar{2}$10] direction between two long chains may induce significant changes of the CO_2 vibration frequencies in Fig. 4 due to the interchain interaction.

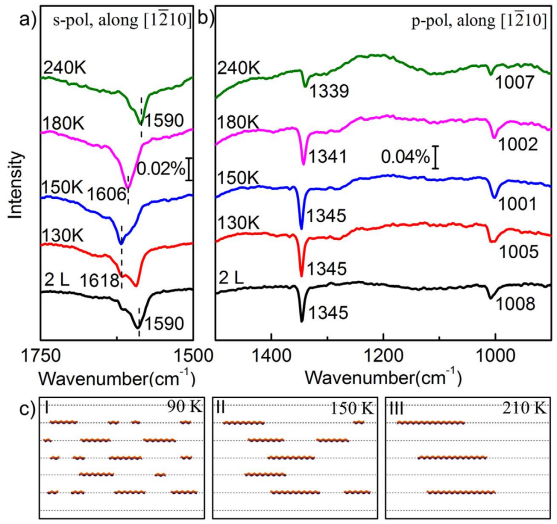

Figure 4. IRRA spectra of saturated adsorbed CO_2 (0.7 ML) on ZnO(10$\bar{1}$0) surfaces with annealing by using (**a**) s-polarized and (**b**) p-polarized IR beams, respectively. The IR light incident is along [1$\bar{2}$10] direction. All spectra were acquired at 90 K. (**c**) Schematic kinetic model to illustrate the mechanism of the phase evolution during annealing. The zigzag lines denote the different lengths of CO_2 chains.

Thereafter, we calculated a series of CO_2 long chains with different interchain distances, such as the isolated long chain, two neighbouring chains (corresponding to (1×1) phase) with the shortest distance of a_0, and two spacing chains (corresponding to (2×1) phase) with $2a_0$. Here a_0 represents the lattice constant along [1$\bar{2}$10] direction of ZnO(10$\bar{1}$0) surfaces. The calculated results are shown in Table 1. We found that the calculated ν_{as} of the spacing chains is 1574 cm^{-1}, which is consistent with the experimental 1590 cm^{-1} at 90 K and 240 K. The calculated ν_s of these spacing chains is 1303 cm^{-1}, which is in agreement with the vibration frequencies of 1345 cm^{-1} at 90 K and 240 K. These obviously indicate that the experimentally observed vibration bands at both 90 K and 240 K belong to the spacing chains. Similarly, the experimentally observed vibration frequencies at 150 K belong to the neighbouring chains.

In Fig. 4c, we give a schematic evolution picture of the CO_2 chains with increasing temperature. At low temperature of 90 K, on the one hand, the CO_2 chains with various length are randomly distributed on the surface due to the low kinetic energy; on the other hand, most of the interchain spaces along [1$\bar{2}$10] are equal to $2a_0$ caused by the interchain repulsion, forming the local (2×1) phase, as shown in Fig. 4c-I. Annealing to 150 K, the CO_2 diffusion is enhanced to induce the Ostwald ripening between CO_2 chains: the CO_2 molecules detach from the short chains and attach to the long ones. Finally, the lengthened chains become neighbouring with others, forming the local (1×1) phase, as shown in Fig. 4c-II. However, due to the strong repulsive interaction between neighbouring chains, the (1×1) phase is an unstable intermediate state. Further annealing the intermediate state to 240 K, all the chains will relax to the more stable spacing structure, forming the well-defined stable (2×1) phase, as shown in Fig. 4c-III.

Conclusion

In conclusion, the formation and evolution of CO_2 chains on ZnO(10$\bar{1}$0) surfaces was studied by employing UHV-FTIRS and DFT calculations. We observed the fine structures of CO_2 vibrational levels on ZnO(10$\bar{1}$0) surfaces, which are attributed to the formation of CO_2 monomer, dimer, trimer and longer polymer chains along [0001] direction. At high CO_2 coverage, the as-grown local (2×1) phase composed of chains with various lengths further evolve into the unstable local (1×1) phase with annealing to 150 K, and then relax into the well-defined stable (2×1) phase above 150 K. The mechanisms of the chain formation and evolution were discussed by DFT calculations and a schematic kinetic model.

Methods

Experimental details. The experiments were carried out using an ultrahigh vacuum (UHV) system[17] (the base pressure better than 6×10^{-11} mbar) equipped with a vacuum Fourier transform infrared spectroscopy (FTIR) spectrometer (Bruker, VERTEX 80 v), a low energy electron diffraction (LEED)/Auger (AES) spectrometer with gain power of microchannel plates BDL 600IR-MCP. The clean mix-terminated ZnO(10$\bar{1}$0) ($8 \times 8 \times 1$ mm, MTI) surface was prepared by repeated cycles of Ar^+ sputtering and annealing at 800 K under UHV conditions until no impurities were detected by AES and clear (1×1) LEED patterns were obtained. Then, the clean ZnO(10$\bar{1}$0) was oxidized in oxygen atmosphere (5×10^{-7} mbar) at 750 K for 20 minutes. The IR measurements were performed using infrared reflection absorption spectroscopy (IRRAS) mode with a fixed incidence angle of 80°. The recorded data, i.e., the absorbance is defined as $A = \log_{10}(R_0/R)$, where R_0 and R are the reflected signals from the bare and the adsorbate covered surfaces, respectively. The optical path was evacuated in order to avoid any unwanted IR adsorption from gas phase species. High purity CO_2 (99.99%) and O_2 (99.999%) were dosed via backfilling in the experiments.

Computational details. First-principles calculations were performed using the Vienna ab-initio simulation package (VASP)[27,28] with a cut-off energy of 500 eV for the basis set. Γ-point was used for Brillouin zone sampling. The projector-augmented wave method (PAW)[29] with the PBE type exchange–correlation potentials[30] was adopted. To model the ZnO(10$\bar{1}$0) surface, the optimized lattice parameters of bulk ZnO, a = 3.285 Å and c/a = 1.6131, were used to build slabs with six ZnO layers. Two surface unit cells, which have dimensions of 6×2 and 2×4 along[0001] and [1$\bar{2}$10] directions, respectively, were employed to perform the calculations. The atomic positions of top three layers were optimized until the forces are less than 0.03 eV/Å, while the bottom layers were fixed at bulk positions. A vacuum layer with a thickness of 15 Å was used to minimize interactions between adjacent slabs. The vibrational frequencies were derived from Hessian matrix calculated by finite-displacement method.

References

1. Thomas, J. M. & Thomas, W. J. *Principles and Practices of Heterogeneous Catalysis*. (VCH, Weinheim (1997).
2. Kurtz, M. *et al.* Active Sites on Oxide Surfaces: ZnO-catalyzed Synthesis of Methanol from CO and H_2. *Angew. Chem. Int. Ed.* **44,** 2790–2794 (2005).
3. Wöll, C. The Chemistry and Physics of Zinc Oxide Surfaces. *Prog. Surf. Sci.* **82,** 55–120 (2007).
4. Burghaus, U. Surface Chemistry of CO_2 – Adsorption of Carbon Dioxide on Clean Surfaces at Ultrahigh Vacuum. *Prog. Surf. Sci.* **89,** 161–217 (2014).
5. Wang, Y. *et al.* CO_2 Activation by ZnO through the Formation of an Unusual Tridentate Surface Carbonate. *Angew. Chem. Int. Ed.* **46,** 5624–5627 (2007).
6. Buchholz, M., Weidler, P. G., Bebensee, F., Nefedov, A. & Woll, C. Carbon Dioxide Adsorption on a ZnO(10$\bar{1}$0) Substrate Studied by Infrared Reflection Absorption Spectroscopy. *Phys. Chem. Chem. Phys.* **16,** 1672–1678 (2014).
7. Scarano, D., Spoto, G., Bordiga, S., Zecchina, A. & Lamberti, C. Lateral Interactions in CO Adlayers on Prismatic ZnO faces: a FTIR and HRTEM study. *Surf. Sci.* **276,** 281–298 (1992).
8. Dulub, O., Meyer, B. & Diebold, U. Observation of the Dynamical Change in a Water Monolayer Adsorbed on a ZnO Surface. *Phys. Rev. Lett.* **95,** 136101 (2005).
9. Wang, Y. *et al.* Hydrogen Induced Metallicity on the ZnO(10$\bar{1}$0) Surface. *Phys. Rev. Lett.* **95,** 266104 (2005).
10. Davis, R. *et al.* The Orientation of Formate and Carbonate on ZnO(10$\bar{1}$0). Surf. *Sci.* **298,** L196–L202 (1993).
11. Wang, Y. *et al.* Tuning the Reactivity of Oxide Surfaces by Charge-Accepting Adsorbates. *Angrew. Chem. Int. Ed.* **46,** 7315–7318 (2007).
12. Noei, H., Wöll, C., Muhler, M. & Wang, Y. The Interaction of Carbon Monoxide with Clean and Surface-modified Zinc Oxide Nanoparticles: A UHV-FTIRS study. *Appl. Catal. A: Gen.* **391,** 31–35 (2011).
13. Heidberg, J. *et al.* Vibrational Infrared Spectra of Adsorbates on Ionic Single Crystal Surfaces: CO_2 on NaCl(100). *Vacuum.* **38,** 275–277 (1988).
14. Heidberg, J.; Kampshoff, E. & Suhren, M. Correlation Field, Structure, and Phase Transtion in the Monolayer CO Adsorbed on NaCl(100) as Revealed from Polarization Fourier-transform Infrared Spectroscpy. *J. Chem. Phys.* **95,** 9408 (1991).
15. Heidberg, J. & Meine, D. Polarized Infrared Spectra of CO_2 Adsorbed on the MgO(100) Single Crystal Surface. *Surf. Sci. Lett.* **279,** L175–L179, (1992).
16. Heidberg, J., Kandel, M., Merine, D. & Wildt, U. The Monolayer CO Adsorbed on MgO(100) Detected by Polarizatin Infrared Spectroscopy. *Surf. Sci.* **331,** 1467–1472 (1995).
17. Cao, Y. J., Hu, S. J., Yu, M., Yan, S. S. & Xu, M. C. Adsorption and Interaction of CO_2 on Rutile TiO_2(110) Surfaces: A Combined UHV-FTIRS and Theoretical Simulation Study. *Phys. Chem. Chem. Phys.* **17,** 23994–4000 (2015).
18. Chabal, Y. Surface Infrared Spectroscopy. *Surf. Sci. Rep.* **8,** 211–357 (1988).
19. Noei, H., Wöll, C., Muhler, M. & Wang, Y. Activation of Carbon Dioxide on ZnO Nanoparticles Studied by Vibrational Spectroscopy. *J. Phys. Chem. C* **115,** 908–914 (2011).
20. Shao, X., Fukui, K.-i., Kondoh, H., Shionoya, M. & Iwasawa, Y. STM Study of Surface Species Formed by Methanol Adsorption on Stoichiometric and Reduced ZnO(10$\bar{1}$0) Surfaces. *J. Phys. Chem. C.* **113,** 14356–14362 (2009).
21. Shi, H. *et al.* Directional Growth of One-Dimensional CO_2 Chains on ZnO(10$\bar{1}$0). *J. Phys. Chem. C.* **120,** 23669–23674 (2016).
22. Zhao, X. *et al.* Formation of Water Chains on CaO(001): What Drives the 1D Growth? *J Phys. Chem. Lett.* **6,** 1204–1208 (2015).
23. Zhong, D. *et al.* Linear Alkane Polymerization on a Gold Surface. *Science* **334,** 213–216 (2011).
24. Lin, T., Shang, X. S., Adisoejoso, J., Liu, P. N. & Lin, N. Steering on-surface Polymerization with Metal-directed Template. *J. Am. Chem. Soc.* **135,** 3576–3582 (2013).
25. Gambardella, P. *et al.* Oscillatory Magnetic Anisotropy in One-Dimensional Atomic Wires. *Phys. Rev. Lett.* **93,** 077203 (2004).
26. Donadio, D., Ghiringhelli, L. M. & Delle Site, L. Autocatalytic and Cooperatively Stabilized Dissociation of Water on a Stepped Platinum Surface. *J. Am. Chem. Soc.* **134,** 19217–19222 (2012).
27. Kresse, G. & Hafner, J. Ab initio Molecular Dynamics for Liquid Metals. *Phys. Rev. B.* **47,** 558–561 (1993).
28. Kresse, G. & Hafner, J. Ab initio Molecular-dynamics Simulation of the Liquid-metal-amorphous Semiconductor Transition in Germanium. *Phys. Rev. B.* **49,** 14251–14269 (1994).
29. Blöchl, P. E. Projector Augmented-wave Method. *Phys. Rev. B.* **50,** 17953–17979 (1994).
30. Perdew, J. P., Burke, K. & Ernzerhof, M. Generalized Gradient Approximation Made Simple. *Phys. Rev. Lett.* **77,** 3865–3868 (1996).

Acknowledgements

This work was supported by the National Science Foundation of China (Grant Nos 21273132 and 11504203) and 111 project B13029.

Author Contributions

Y.J.C. and M.C.X. designed the research. Y.J.C., Y.M., S.D.Q., T.T.W. and S.M.H. conducted the IRRAS experiments. S.J.H. performed the theoretical calculations. Y.J.C., M.C.X., S.J.H. and S.S.Y. contributed to writing and revising the manuscript.

Additional Information

Supplementary information accompanies this paper at http://www.nature.com/srep

Competing financial interests: The authors declare no competing financial interests.

How to cite this article: Cao, Y. *et al.* Formation and evolution of orientation-specific CO_2 chains on nonpolar ZnO(10$\bar{1}$0) surfaces. *Sci. Rep.* **7**, 43442; doi: 10.1038/srep43442 (2017).